Nanoscale Research Letters

NANO EXPRESS Open Access

Optimization of InGaAs/InAlAs Avalanche Photodiodes

Jun Chen[1*], Zhengyu Zhang[1], Min Zhu[1], Jintong Xu[2] and Xiangyang Li[2]

Abstract

In this paper, we report a two-dimensional (2D) simulation for InGaAs/InAlAs separate absorption, grading, charge, and multiplication avalanche photodiodes (SAGCM APDs) and study the effect of the charge layer and multiplication layer on the operating voltage ranges of APD. We find that with the increase of the thicknesses as well as the doping concentrations of the charge layer and the multiplication layer, the punchthrough voltage increases; with the increase of the doping concentrations of two layers and the thickness of the charge layer, the breakdown voltage decreases; with the increase of the thickness of the multiplication layer, the breakdown voltage first rapidly declines and then slightly rises.

Keywords: Avalanche photodiodes (APDs), Punchthrough voltage, Breakdown voltage, Simulation

Background

Focal plane array (FPA) based on $In_{0.53}Ga_{0.47}As$ (referred as InGaAs hereafter) has a huge market and wide application prospect, and it is widely used in military field [1]. For narrow band gap materials like InGaAs, high tunneling current limits their usefulness. Separating the absorption and multiplication layer can overcome this disadvantage [2]. InGaAs is often used to absorb light at a wavelength of 1.55 μm, while for the multiplication layer, $In_{0.52}Al_{0.48}As$ (referred as InAlAs hereafter) is a good multiplication layer material [3]. InAlAs has been demonstrated to be a good electron multiplication material for InGaAs separate absorption and multiplication avalanche photodiodes (SAM APDs) because of its low electron impact ionization threshold energy of 1.9–2.2 eV, high ionization coefficient ratio of electron to hole than that of hole to electron in InP, and small excess noise factor [4, 5].

For separate absorption, grading, charge, and multiplication avalanche photodiodes (SAGCM APDs), the key issue is to adjust the electric field distribution in the device by changing the thickness and doping concentration of the charge layer and the multiplication layer. Provided that the electric field is sufficiently large in the multiplication region, the carriers will undergo avalanche multiplication, and the device behaves as an avalanche photodetectors (APD) as desired [6]. The SAGCM structure allows independent control of the parameters of the charge layer and the multiplication layer (thickness and the doping concentration). In this paper, we study the effect of the charge layer and multiplication layer on the operating voltage ranges of APD and analyze the results theoretically from the internal electric field distribution.

Methods

Figure 1 shows the schematic cross-section of a top-illuminated SAGCM InGaAs/InAlAs APD with 400 μm^2 mesa structure. From the top to the bottom, these layers are sequentially named as contact layer, window layer, absorption layer, grading layer, charge layer, multiplication layer, InAlAs buffer layer, InP buffer layer, and InP substrate. The device structure in our simulation is the same as the experimental device reported in Ref. [7].

The steady-state two-dimensional (2D) numerical simulations are performed for the top-illuminated SAGCM InGaAs/InAlAs APD by using Silvaco TCAD [8]. The Shockley–Read–Hall (SRH), auger, band-to-band tunneling, and trap-assisted tunneling models are used in our simulation. The generation rate G_{bbt} of band-to-band tunnel is described in Eqs. (1) and (2) [8].

* Correspondence: junchen@suda.edu.cn
[1]School of Electronic and Information Engineering, Soochow University, Suzhou 215006, China
Full list of author information is available at the end of the article

Springer Open

© The Author(s). 2017 **Open Access** This article is distributed under the terms of the Creative Commons Attribution 4.0 International License (http://creativecommons.org/licenses/by/4.0/), which permits unrestricted use, distribution, and reproduction in any medium, provided you give appropriate credit to the original author(s) and the source, provide a link to the Creative Commons license, and indicate if changes were made.

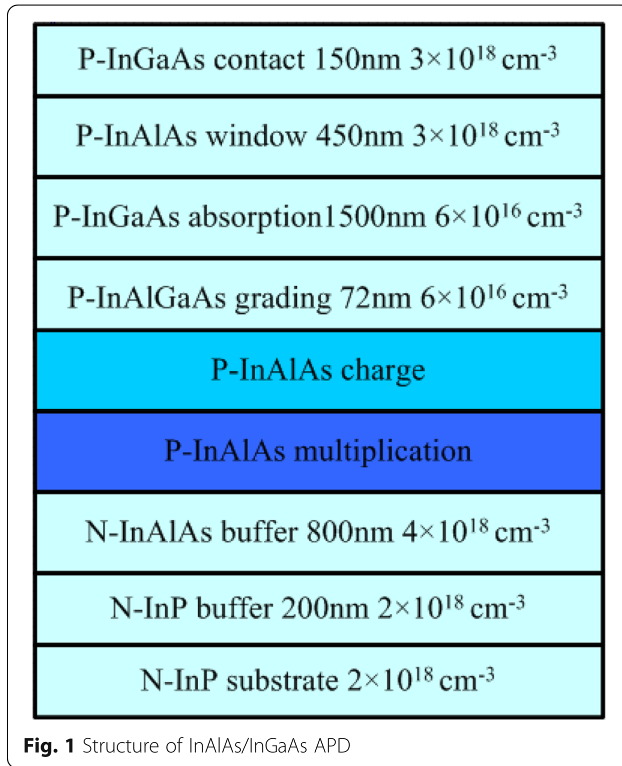

Fig. 1 Structure of InAlAs/InGaAs APD

$$G_{\mathrm{bbt}} = A \cdot E \cdot \exp\left(-\frac{B}{E}\right) \tag{1}$$

$$A = -\frac{q^2\sqrt{2m_e^*}}{4\pi^3 h^2\sqrt{E_g}} \qquad B = \frac{\pi\sqrt{m_e^*/2}E_g^{3/2}}{2q\hbar} \tag{2}$$

The A and B are the characterization parameters; E is the magnitude of electric field, and E_{g} is the band gap energy level. The generation rate R_{tat} in trap-assisted tunneling process is given in Eqs. (3)–(5) [8–11].

$$R_{\mathrm{tat}} = \frac{pn - n_{\mathrm{i}}^2}{\frac{\tau_p}{1+\Gamma_p}\left[n + n_{\mathrm{i}} \cdot \exp\left(\frac{E_{\mathrm{t}}-E_{\mathrm{i}}}{kT}\right)\right] + \frac{\tau_n}{1+\Gamma_n}\left[p + n_{\mathrm{i}} \cdot \exp\left(\frac{E_{\mathrm{i}}-E_{\mathrm{t}}}{kT}\right)\right]} \tag{3}$$

$$\Gamma_{n,p} = \frac{\Delta E_{n,p}}{kT}\int_0^1 \exp\left(\frac{\Delta E_{n,p}}{kT}u - K_{n,p}u^{3/2}\right)du \tag{4}$$

$$K_{n,p} = \frac{4}{3}\frac{\sqrt{2m_{\mathrm{trap}}(\Delta E_{n,p})^3}}{3qh|E|} \tag{5}$$

where τ_n (τ_p) is the electron (hole) lifetime due to the SRH recombination. E_{t} is the trap level, and N_{t} is the trap concentration. E_{i} is the intrinsic Fermi level, and n_{i} is the intrinsic carrier concentration. Γ_n (Γ_p) is the enhancement factor and includes the effects of field-assisted tunneling on the emission of electrons (holes) from a trap, ΔE_n (ΔE_p) is the energy range where tunneling can occur for electrons (holes), u is the integration variable, and m_{trap} is the effective mass used for carrier tunneling. The effect of carrier avalanche is accounted for by the impact ionization model, which has the following forms:

$$G^{ava} = \alpha_n n v_n + \alpha_p p v_p \tag{6}$$

Where $\alpha_{n,p}$ are the electron and hole ionization coefficients, respectively, [8, 12, 13]

$$\alpha_{n,p}(F) = \gamma a_{n,p} e^{\frac{-\gamma b_{n,p}}{F}} \tag{7}$$

The parameters above are listed in Table 1.

Results and Discussion

Figure 2 presents the simulated and experimental current–voltage (I–V) characteristics for the top-illuminated SAGCM InGaAs/InAlAs APD. The simulated results are in good agreement with the experimental data reported in Ref. [7].

The simulated I–V characteristics at different doping concentrations of the multiplication layer are shown in Fig. 3, the punchthrough voltage (at the unity gain point: the bias where the responsivity of APD reaches ~0.6 A/W) increases monotonically with the increasing of doping concentration ($4 \times 10^{16} \sim 1.5 \times 10^{16}$ cm^{-3}), [14] while the breakdown voltage (dark current ~ 1×10^{-5} A) decreases monotonically. With the change of the doping concentration, the electric field in the multiplication layer changes obviously. We analyze the results theoretically following assumptions and simplifications [15]:

1. P^+–N is an abrupt junction
2. The doping concentrations in the multiplication, charge, grading and absorption layers are uniform
3. If the absorption layer is completely depleted at breakdown voltage, x_{s} will be the thickness of the absorption layer

Table 1 Material parameters used for InGaAs/InAlAs APD simulation [6, 8, 16, 17]

Parameters/InAlAs	Units	Electron	Hole
SRH lifetime	s	1×10^{-6}	1×10^{-6}
Radioactive coefficient	cm^3 s^{-1}	1.2×10^{-10}	1.2×10^{-10}
BBT coefficient α	1	2	2
BBT coefficient A	1/V cm s	2.1×10^{11}	2.2×10^{6}
BBT coefficient B	V/cm	2.1×10^{11}	2.2×10^{6}
Trap level E_{t}	ev	0.72	
Trap concentrations N_{t}	cm^{-3}	1×10^{-12}	
m_{trap}	m_0	0.03	
Impact coefficient a	cm^{-1}	1.3×10^{7}	3.3×10^{7}
Impact coefficient b	V/cm	3.5×10^{6}	4.5×10^{6}

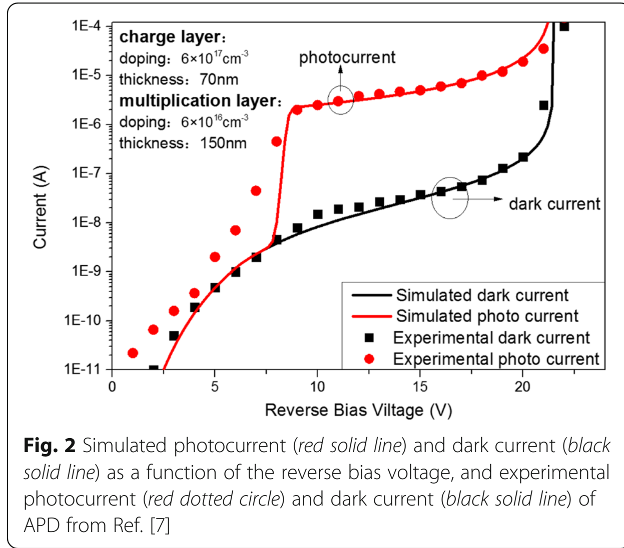

Fig. 2 Simulated photocurrent (*red solid line*) and dark current (*black solid line*) as a function of the reverse bias voltage, and experimental photocurrent (*red dotted circle*) and dark current (*black solid line*) of APD from Ref. [7]

$$V_{\mathrm{mesa}} + V_{\mathrm{bi}} = \frac{q\sigma_{\mathrm{m}}}{\varepsilon_1\varepsilon_0}\left(\frac{x_{\mathrm{m}}}{2}\right) + \frac{q\sigma_{\mathrm{c}}}{\varepsilon_1\varepsilon_0}\left(x_{\mathrm{m}} + \frac{x_{\mathrm{c}}}{2}\right) + \frac{q\sigma_{\mathrm{g}}}{\varepsilon_2\varepsilon_0}\left(x_{\mathrm{m}} + x_{\mathrm{c}} + \frac{x_{\mathrm{g}}}{2}\right) \quad (8)$$

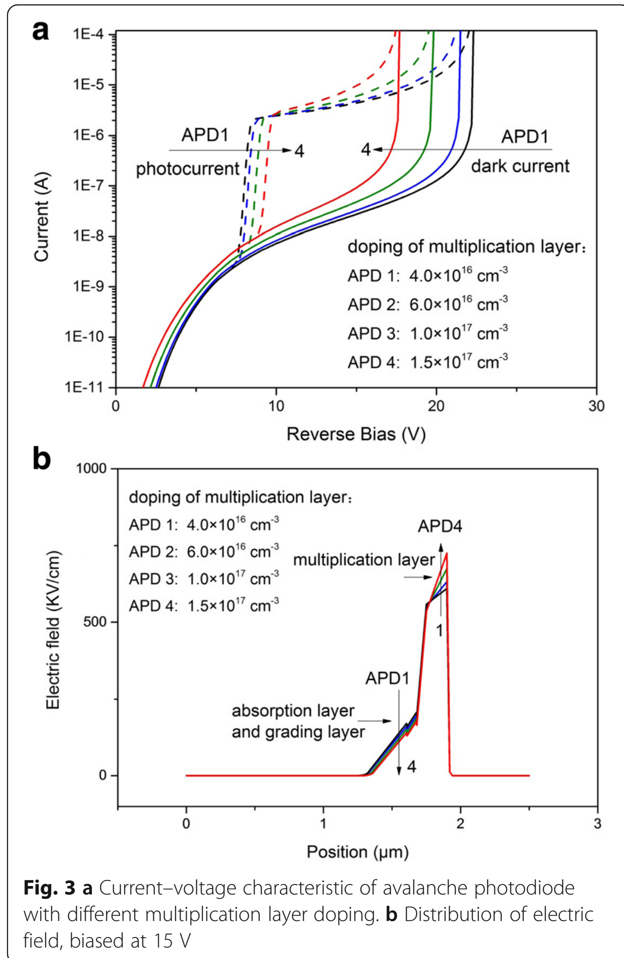

Fig. 3 **a** Current–voltage characteristic of avalanche photodiode with different multiplication layer doping. **b** Distribution of electric field, biased at 15 V

$$\begin{aligned} V_{\mathrm{br}} + V_{\mathrm{bi}} = {} & F_{\mathrm{br}}\left(x_{\mathrm{m}} + x_{\mathrm{c}} + x_{\mathrm{g}} + x_{\mathrm{s}}\right) \\ & - \frac{q\sigma_{\mathrm{m}}}{\varepsilon_1\varepsilon_0}\left(\frac{x_{\mathrm{m}}}{2} + x_{\mathrm{c}} + x_{\mathrm{g}} + x_{\mathrm{s}}\right) - \frac{q\sigma_{\mathrm{c}}}{\varepsilon_1\varepsilon_0}\left(\frac{x_{\mathrm{c}}}{2} + x_{\mathrm{g}} + x_{\mathrm{s}}\right) \\ & - \frac{q\sigma_{\mathrm{g}}}{\varepsilon_2\varepsilon_0}\left(\frac{x_{\mathrm{g}}}{2} + x_{\mathrm{s}}\right) - \frac{q\sigma_{\mathrm{s}}}{\varepsilon_3\varepsilon_0}x_{\mathrm{s}} \end{aligned} \quad (9)$$

The V_{mesa} is the punchthrough voltage, V_{bi} is the zero bias voltage, and V_{br} is the breakdown voltage; x_{m}, x_{c}, and x_{g} are the thickness of the multiplication, charge, and grading layer, respectively; and σ_{m}, σ_{c}, σ_{g}, and σ_{s} are the charge density in the multiplication, charge, grading, and absorption layer, respectively, $\sigma = N \cdot x$; and ε_0, ε_1, ε_2, and ε_3 are the dielectric constant of vacuum, InAlAs, InGaAs, InAlGaAs, respectively; F_{br} is the electric field in the multiplication layer at breakdown [13]. To get smaller dark currents, larger breakdown voltage, and larger gain factor, the doping of absorption layer is relatively higher [14]. From Eq. (9), when the absorption layer is not completely depleted at breakdown voltage, x_{s} is the width of the depletion region of the InGaAs absorption layer.

With the decreasing of doping concentration, the electric field between the absorption layer and the grading layer increases, which makes the electron more easier to punch through the absorption layer and the grading layers, so the punchthrough voltage decreases, owing to the wedge-shaped electric field profile with a high gradient [12]. From Fig. 3, we can see that the doping of the multiplication layer has a great influence on the performance of the device.

Figure 4 shows the simulated I–V characteristics with different thicknesses of the multiplication layer (0.05 ~ 0.25 μm). The punchthrough voltage increases with the increasing thickness of multiplication layer, [13] and the breakdown voltage first rapidly declines then slightly rises (Fig. 5). We analyze the results theoretically from Eqs. (8) and (9), and the following equations: [18]

$$M_n = \frac{1-1/k}{\exp[-\alpha(1-1/k)x_{\mathrm{m}}]-1/k} \quad (10)$$

(M_n is the multiplication factor of electron in the multiplication layer)

So, we can get:

$$\frac{\partial M_n}{\partial x_{\mathrm{m}}} = M_n^2\left(\alpha + x_{\mathrm{m}}\frac{\partial \alpha}{\partial x_{\mathrm{m}}}\right)\exp[-\alpha(1-1/k)x_{\mathrm{m}}] \quad (11)$$

$$\frac{\partial \alpha}{\partial x_{\mathrm{m}}} = \frac{\partial \alpha}{\partial E_{\mathrm{m}}}\frac{\partial E_{\mathrm{m}}}{\partial x_{\mathrm{m}}} \quad (12)$$

(E_{m} is the max electric field intensity in the multiplication layer).

So,

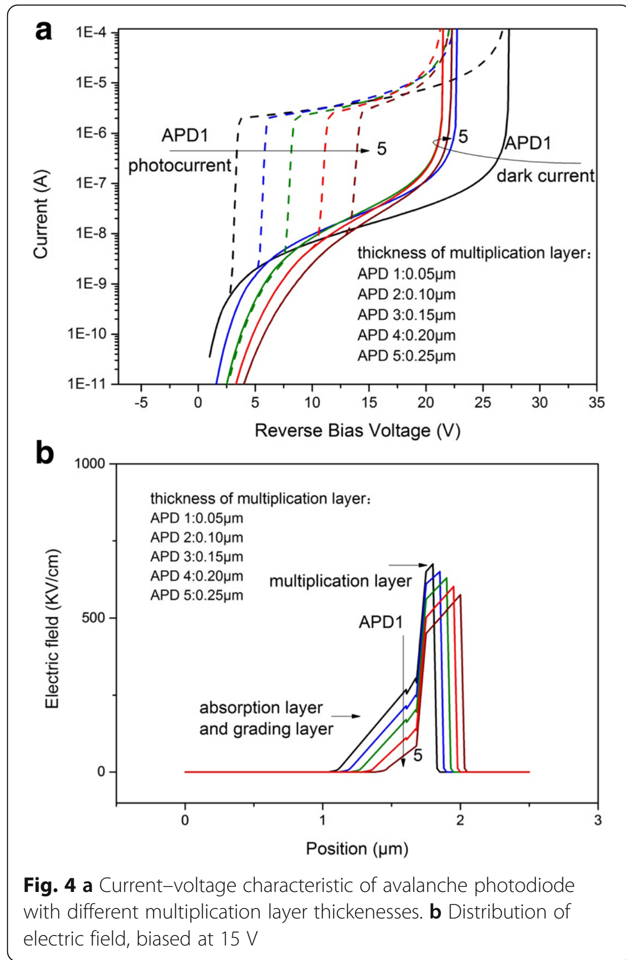

Fig. 4 a Current–voltage characteristic of avalanche photodiode with different multiplication layer thickenesses. **b** Distribution of electric field, biased at 15 V

$$x_{\mathrm{m}} > \frac{-\alpha}{\partial\alpha/\partial x_{\mathrm{m}}} \Rightarrow \alpha + x_{\mathrm{m}}\frac{\partial\alpha}{\partial x_{\mathrm{m}}} < 0 \Rightarrow \frac{\partial M_n}{\partial x_{\mathrm{m}}} < 0,$$

$$x_{\mathrm{m}} < \frac{-\alpha}{\partial\alpha/\partial x_{\mathrm{m}}} \Rightarrow \alpha + x_{\mathrm{m}}\frac{\partial\alpha}{\partial x_{\mathrm{m}}} > 0 \Rightarrow \frac{\partial M_n}{\partial x_{\mathrm{m}}} > 0,$$

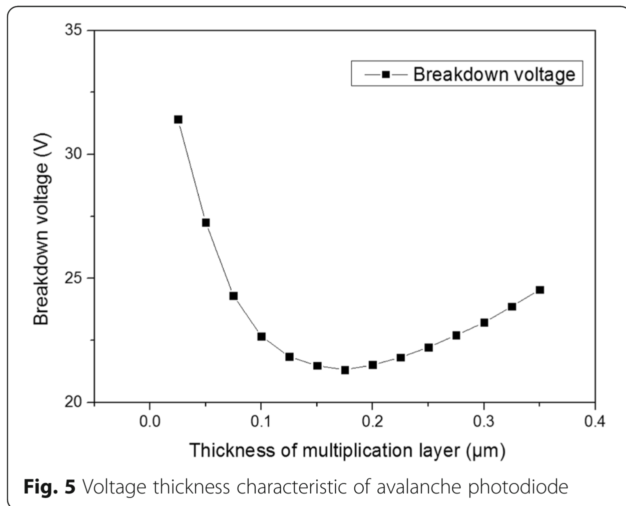

Fig. 5 Voltage thickness characteristic of avalanche photodiode

The above equations explain that when the multiplication layer thickness x_{m} is smaller than the critical point $\frac{-\alpha}{\partial\alpha/\partial x_{\mathrm{m}}}$, the breakdown voltage declines. When x_{m} is larger than that point, the breakdown voltage slightly rises. The value of the critical point calculated from the Eqs. (10)–(12) is ~ 0.2 μm, which is close to the simulated result in Fig. 5.

From the electric field distribution, with the increasing thickness of multiplication layer, the electric field in the absorption layer and the grading layer decreases, making the electrons more difficult to punch through the layers, so the punchthrough voltage increases. From the simulation results, in order to get a larger operating voltage range, the doping and thickness of the multiplication layer can be 4×10^{16} cm^{-3} and 0.05 μm, respectively.

The electric field in the multiplication layer is enhanced by the charge layer to ensure the multiplication effect occurs in the multiplication layer. The thickness and the doping concentration of the charge layer can control the electric field in the multiplication layer. Figure 6 shows the dark and illuminated current characteristics with different doping concentrations

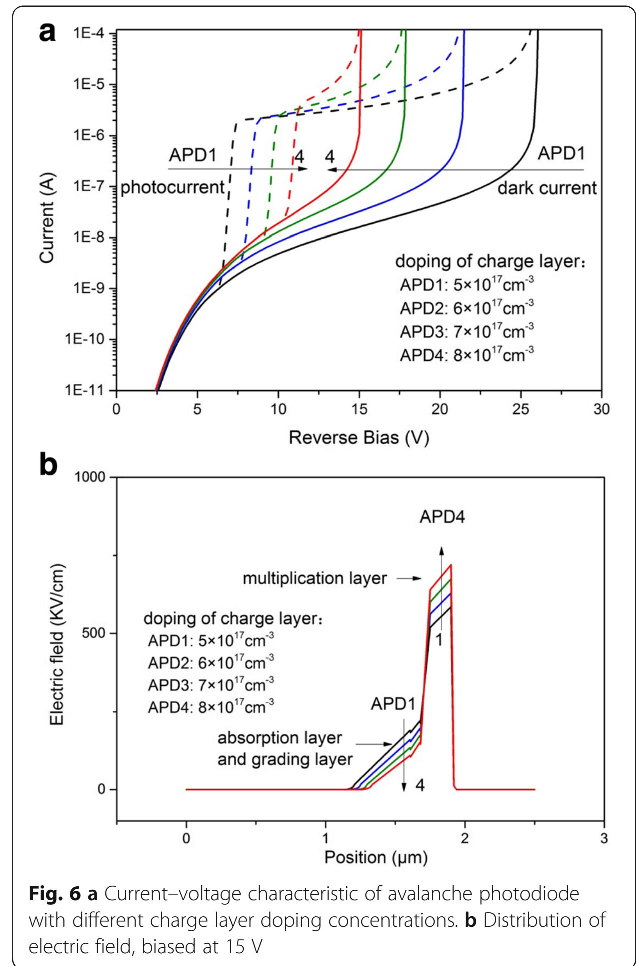

Fig. 6 a Current–voltage characteristic of avalanche photodiode with different charge layer doping concentrations. **b** Distribution of electric field, biased at 15 V

($5 \times 10^{17} \sim 8 \times 10^{17}$ cm^{-3}). With the increasing of doping concentration, the punchthrough voltage increases and the breakdown voltage decreases. Figure 7 shows the *I*–*V* characteristics with different thicknesses of the charge layer, and we can observe that with the increasing thickness, the punchthrough voltage increases while the breakdown voltage decreases [19, 20]. With the increasing thickness and the doping of charge layer, the electric field in the absorption layer and the grading layer decreases, and it makes the electron more difficult to punch through the layers, so the punchthrough voltage increases, but the electric field in multiplication layer increases with the increased thickness and the doping of charge layer. The thickness and doping concentration of the charge layer only affect the voltage distribution in the APD, so with the change of the parameters, the punchthrough voltage and the breakdown voltage change monotonously. Based on the simulation results, to further increase the operating voltage range, the doping and thickness of the charge layer can be 5×10^{17} cm^{-3} and 0.065 μm, respectively.

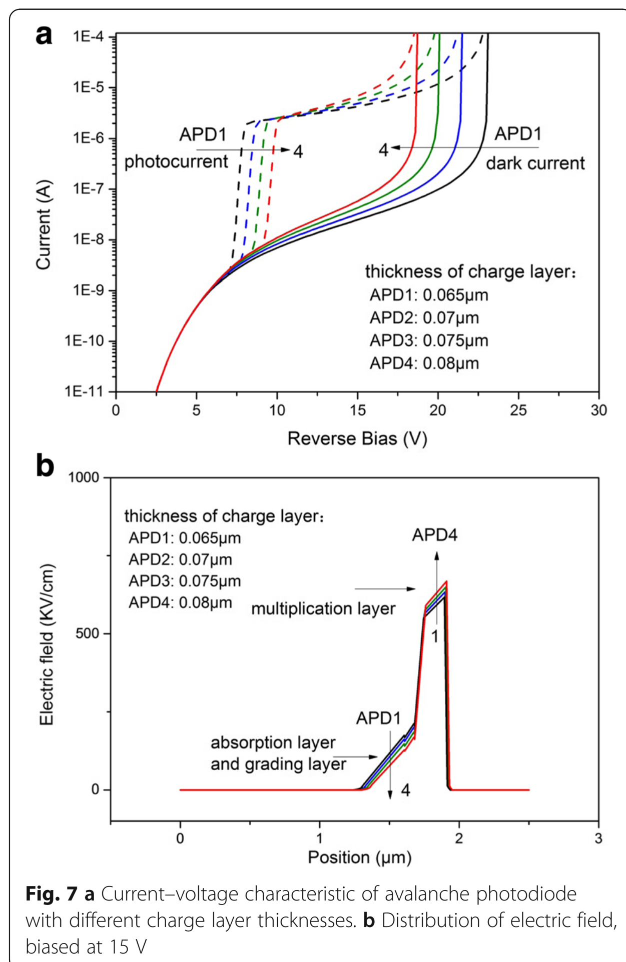

Fig. 7 a Current–voltage characteristic of avalanche photodiode with different charge layer thicknesses. **b** Distribution of electric field, biased at 15 V

Conclusions

In summary, we simulated and analyzed the punchthrough voltage and the breakdown voltage with the change of the parameters of the charge layer and multiplication layer. We found that with the increase of the thicknesses and the doping concentrations of the charge layer and the multiplication layer, the punchthrough voltage increases; with the increase of the doping concentrations of two layers and the thickness of the charge layer, the breakdown voltage decreases; with the increase of the thickness of the multiplication layer, the breakdown voltage first rapidly declines then slightly rises. Results show that the range of the operating voltage can be changed significantly by the charge layer and multiplication layer.

Abbreviations

2D: Two-dimensional; FPA: Focal plane array; *I–V*: Current–voltage; SAGCM APDs: Separate absorption, grading, charge, and multiplication avalanche photodiodes; SAM APDs: Separate absorption and multiplication avalanche photodiodes; SRH: Shockley–Read–Hall

Funding

This project is partially supported by the National Natural Science Foundation of China (61307044), the Natural Science Foundation of Jiangsu Province of China (BK20130321), the Research Fund for the Doctoral Program of Higher Education of China (20133201120009), the open project of Key Laboratory of Infrared Imaging Materials and Detectors, Chinese Academy of Sciences (IIMDKFJJ-15-06), the Scientific Research Foundation for the Returned Overseas Chinese Scholars, Ministry of Education of China, and the Research Innovation Program for College Graduates of Jiangsu Province (SJLX15-0601).

Authors' Contributions

JC initiated the research, designed the modeling strategy, and supervised all the work. JC, ZZ, and MZ carried out the simulation and drafted the manuscript. JX and XL contributed to the data analysis. All authors read and approved the manuscript.

Competing Interests

The authors declare that they have no competing interests.

Author details

[1]School of Electronic and Information Engineering, Soochow University, Suzhou 215006, China. [2]Key Laboratory of Infrared Imaging Materials and Detectors, Shanghai Institute of Technical Physics, Chinese Academy of Sciences, Shanghai 200083, China.

Received: 1 November 2016 Accepted: 27 December 2016
Published online: 13 January 2017

References

1. Martyniuk P, Antoszewski J, Martyniuk M et al (2014) New concepts in infrared photodetector designs. Appl Phys Rev 1(4):041102-1-35
2. Haralson JN, Parks JW, Brennan KF et al. (1997) Numerical simulation of avalanche breakdown within InP-InGaAs SAGCM standoff avalanche photodiodes. Lightwave Technol J 15(11):2137–2140
3. Nakata T, Ishihara J, Makita K et al. (2009) Multiplication noise characterization of InAlAs-APD with heterojunction. Photonics Technol Lett IEEE 21(24):1852–1854
4. Goh YL, Marshall ARJ, Massey DJ et al (2007) Excess avalanche noise in $In_{0.52}Al_{0.48}As$. Quantum Electron IEEE J 43(6):503–507
5. David JPR, Tan CH (2008) Material considerations for avalanche photodiodes. Selected Top Quantum Electron IEEE J 14(4):998–1009
6. Parks JW, Brennan KF, Tarof LE (1998) Macroscopic Device Simulation of InGaAs/InP Based Avalanche Photodiodes. VLSI Design 6(1–4):79–82

7. Ma Y, Zhang Y, Gu Y et al. (2015) Tailoring the performances of low operating voltage InAlAs/InGaAs avalanche photodetectors. Opt Express 23(15):19278–19287
8. Silvaco International (2008) ATLAS User's manual. Silvaco Internat, Santa Clara
9. Kocer H, Arslan Y, Besikci C et al. (2012) Numerical analysis of long wavelength infrared HgCdTe photodiodes. Infrared Phys Technol 55(1):49–55
10. Ferron A, Rothman J, Gravrand O et al. (2013) Modeling of dark current in HgCdTe infrared detectors. Journal of electronic materials 42(11):3303–3308
11. Ji X, Liu B, Xu Y et al (2013) Deep-level traps induced dark currents in extended wavelength $In_xGa_{1-x}As$/InP photodetector. J Appl Phys 114(22): 224502-1-5
12. Qiu WC, Hu WD, Chen L et al. (2015) Dark current transport and avalanche mechanism in HgCdTe electron-avalanche photodiodes. Electron devices. IEEE Transactions on 62(6):1926–1931
13. Wang X, Hu W, Pan M et al (2014) Study of gain and photoresponse characteristics for back-illuminated separate absorption and multiplication GaN avalanche photodiodes. J Appl Phys 115(1):013103-1-8
14. Ma YJ, Zhang YG, Gu Y et al. (2015) Low operating voltage and small gain slope of InGaAs APDs with p-type multiplication layer. Photonics Technol Lett IEEE 27(6):661–664
15. Ma CLF, Deen MJ, Tarof LE et al. (1995) Temperature dependence of breakdown voltages in separate absorption, grading, charge, and multiplication InP/InGaAs avalanche photodiodes. Electron Devices IEEE Trans 42(5):810–818
16. Watanabe I, Torikai T, Makita K et al (1990) Impact ionization rates in (100) $Al_{0.48}In_{0.52}As$. IEEE Electron Device Lett 11(10):437–438
17. Watanabe I, Torikai T, Taguchi K (1995) Monte Carlo simulation of impact ionization rates in InAlAs-InGaAs square and graded barrier superlattice. IEEE J Quantum Electron 31(10):1826–1834
18. Willardson RK, Beed AC (1977) Semiconductors and semimetals. Academic press, New York
19. Zhao Y, He S et al. (2006) Multiplication characteristics of InP/InGaAs avalanche photodiodes with a thicker charge layer. Opt Commun 265(2):476–480
20. Zak D, Jureńczyk J, Kaniewski J et al. (2014) Zener Phenomena in InGaAs/InAlAs/InP Avalanche Photodiodes. Detection 2(2):10–15

Submit your manuscript to a SpringerOpen journal and benefit from:

- ► Convenient online submission
- ► Rigorous peer review
- ► Immediate publication on acceptance
- ► Open access: articles freely available online
- ► High visibility within the field
- ► Retaining the copyright to your article

Submit your next manuscript at ► springeropen.com